ESYWG Exposure Time Calibration Assumptions & Parameters

Christopher C. Stark[a], **Dmitry Savnransky**[b]
[a]NASA Goddard Space Flight Center, 8800 Greenbelt Rd, Greenbelt, MD 20771, USA
[b]Sibley School of Mechanical and Aerospace Engineering, Cornell University, Ithaca, NY 14853, USA

1 Introduction

The Coronagraph Design Survey (CDS), Coronagraph Technology Roadmap (CTR), and the Exoplanet Science Yield sub-Working Group (ESYWG) are three separate studies that all include an exposure time calibration effort as a cross-check on different exoplanet yield codes. As such, we are coordinating the calibration efforts of these three studies.

Here we document the baseline assumptions and parameters used for the exposure time calibration effort. We detail astrophysical assumptions, observational constraints/approaches, and mission performance parameters. Where possible, we build off of the assumptions made during the HabEx and LUVOIR studies[1,2] as well as the CDS study. However, in some cases we intentionally depart from these assumptions to improve the fidelity and/or ease of comparison. E.g., CDS ignored detector noise to ensure yield was driven by coronagraph performance, whereas we include detector noise specifically to check the implementation of these parameters in each code.

2 Methods and baseline assumptions

- OTE
  - We will adopt the off-axis aperture defined by the USORT study as our baseline
  - We adopt a Cassegrain telescope design consistent with Ref. 3 to minimize the number of aluminum reflections and maximize throughput.
  - Optical throughputs for a notional layout are detailed below
- Coronagraphs
  - We will adopt the Optical Vortex Coronagraph simulated by CDS (usort_offaxis_ovc)
  - We will assume perfect WFC
  - We will assume both polarizations can be conducted simultaneously on a single detector (regardless of whether this is possible)
  - We will ignore UV and NIR coronagraph channels for this study.
  - We will assume a single VIS coronagraph channel.
  - We assume separate imaging and spectroscopy modes, with the spectroscopy mode using an IFS with the associated optical throughput reduction
- Detectors
  - We will carry forward the QE (flat 0.9) and dQE (flat 0.75) assumed in Refs. 1, 2
  - We will carry forward all zero detector noise parameters from Refs. 1, 2

- Astrophysics
  - We will adopt a 1 Earth radius planet at quadrature
  - We will assume a Lambertian phase function
  - We will assume the planet is located at the EEID of each star, where the EEID is given by the square root of the bolometric luminosity in solar luminosities
  - We will adopt a geometric albedo of 0.2 that is independent of wavelength
  - We will adopt 3 zodis of dust, where 1 zodi is 22 mags arcsec^{-2}
  - We will include the local zodi
- Observational assumptions
  - For detection time comparisons, we will assume $\lambda = 500$ nm, SNR=7, and 20% coronagraphic bandpass
  - For spectral characterization time, we will TBD
  - We will adopt aperture photometry
  - We will implement a noise floor count rate (using Bijan's prescription)

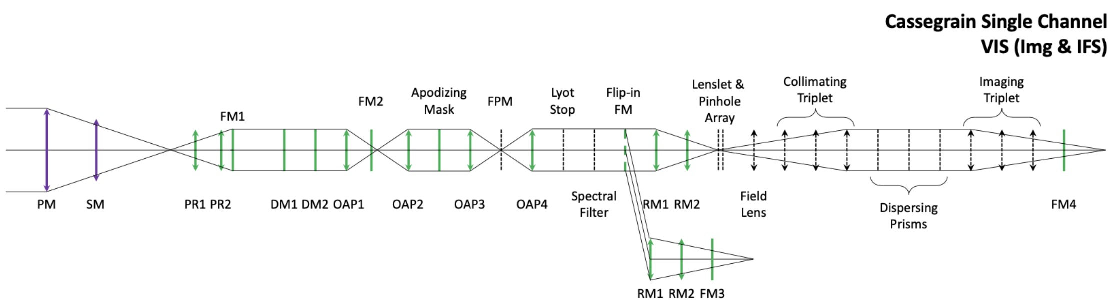

Fig 1 Adopted optical layout for the single VIS coronagraph, with an imager and IFS. This layout was used to calculate the optical throughputs shown in Figure 2.

Table 1. Baseline Astrophysical Parameters

Parameter	Value	Description
$R_{\rm p}$	1.0 $R_\oplus$	ExoEarth candidate radius range
a	1.0 AU	ExoEarth candidate semi-major axis range[a]
e	0	Eccentricity (circular orbits)
θ	$\pi/2$	Phase angle
Φ	Lambertian	Phase function
A_G	0.2	Geometric albedo of exoEarth candidate
z	23 mag arcsec^{-2}	Average V band surface brightness of zodiacal light[b]
z'	22 mag arcsec^{-2}	V band surface brightness of 1 zodi of exozodiacal dust[c]
n	3.0	Exozodi level of each star

[a]For a solar twin. The habitable zone is scaled by $\sqrt{L_\star/L_\odot}$.

[b]Varies with ecliptic latitude.

[c]For Solar twin. Varies with spectral type and planet-star separation—see Appendix C in Ref. 6.

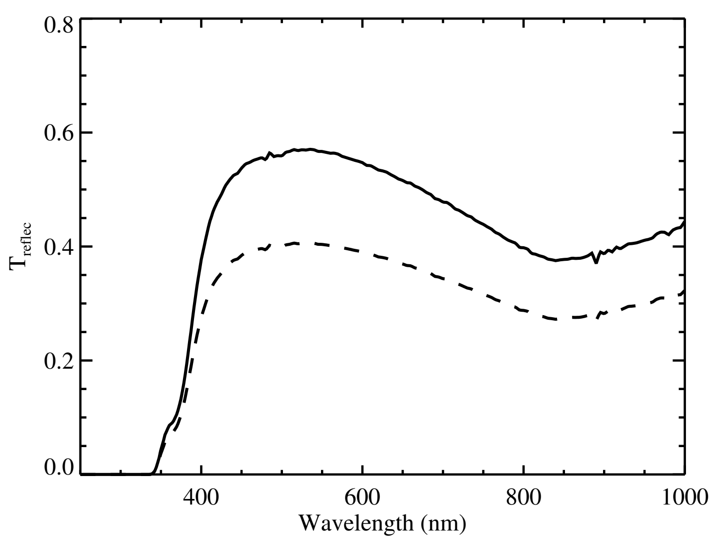

Fig 2 Adopted optical throughput for the VIS coronagraph imager (black solid line) and VIS/NIR IFS (black dashed line). These curves were calculated from the optical layout shown in Figure 1 and used to determine $T_{\rm optical,d}$ and $T_{\rm optical,H2O}$ listed in Table 2.

3 Fiducial stars

We will adopt the five fiducial stars defined by the CTR study:

1. HIP 32439
2. HIP 77052
3. HIP 79672

Table 2. Coronagraph-based Mission Parameters

Parameter	Value	Description
		General Parameters
$\tau_{\rm slew}$	1 hr	Static overhead for slew and settling time
$\tau_{\rm WFC}$	1.3 hrs[a]	Static overhead to dig dark hole
$\tau'_{\rm WFC}$	1.1	Multiplicative overhead to touch up dark hole
D	7.87 m	Telescope circumscribed diameter (USORT aperture)
$D_{\rm ins}$	6.5 m	Telescope inscribed diameter (USORT aperture)
A	Per USORT aperture	Collecting area of telescope (USORT aperture)
X	0.7	Photometric aperture radius in $\lambda/D_{\rm ins}$[b]
Ω	$\pi(X\lambda/D_{\rm ins})^2$ radians	Solid angle subtended by photometric aperture[b]
$\zeta_{\rm floor}$	None	Raw contrast floor enforced regardless of coronagraph design
$\Delta{\rm mag}_{\rm floor}$	26.5	Noise floor (faintest detectable point source at S/N$=10$)
$T_{\rm contam}$	0.95	Effective throughput due to contamination applied to all observations
		Detection Parameters
$\lambda_{\rm d}$	0.5 μm[c]	Central wavelength for detection
$\Delta\lambda_{\rm d}$	20%	Bandwidth assumed for detection
S/N$_{\rm d}$	7	S/N required for detection
$T_{\rm optical,d}$	0.56[c]	End-to-end reflectivity/transmissivity at $\lambda_{\rm d}$
$\theta_{\rm pix,d}$	6.55 mas	scale of detector pixel for detections
		H_2O Characterization Parameters
$\lambda_{\rm H2O}$	1.0 μm[c]	Wavelength for characterization
S/N$_{\rm H2O}$	5[c]	Signal to noise per spectral bin evaluated in continuum
R$_{\rm H2O}$	140	Spectral resolving power
$T_{\rm optical,H2O}$	0.32[c]	End-to-end reflectivity/transmissivity at $\lambda_{\rm H2O}$ including IFS optics
$\theta_{\rm pix,c}$	6.55 mas	scale of detector pixel for characterizations
$\tau_{\rm H2O,limit}$	2 mos	Characterization time limit including overheads
		Detector Parameters
ξ	3×10^{-5} e^- pix^{-1} s^{-1}	Dark current
RN	0 e^- pix^{-1} read^{-1}	Read noise
$\tau_{\rm read}$	1000 s	Time between reads
CIC	1.3×10^{-3} e^- pix^{-1} frame^{-1}	Clock induced charge
$T_{\rm QE}$	0.9	Raw QE of the detector at all wavelengths
$T_{\rm dQE}$	0.75	Effective throughput due to bad pixel/cosmic ray mitigation

[a]For the USORT aperture with VC6 coronagraph and baseline throughput. Same value adopted independent of coronagraph throughput.

[b]$D_{\rm LS}$ is the diameter of Lyot stop projected onto the primary mirror. AYO optimizes this and the associated encircled energy to minimize exposure time on a planet-by-planet basis.

[c]Example provided at most likely bandpass; AYO optimizes bandpass and adjusts values accordingly.

4. HIP 26779
5. HIP 113283

4 Documentation

Exposure time parameters, count rates, and exposure times will all be reported for comparison in a spreadsheet located in the ESYWG's google drive, within the exposure time calibration folder.

References

1 B. S. Gaudi, S. Seager, B. Mennesson, A. Kiessling, K. Warfield, K. Cahoy, J. T. Clarke, S. Domagal-Goldman, L. Feinberg, O. Guyon, J. Kasdin, D. Mawet, P. Plavchan, T. Robinson, L. Rogers, P. Scowen, R. Somerville, K. Stapelfeldt, C. Stark, D. Stern, M. Turnbull, R. Amini, G. Kuan, S. Martin, R. Morgan, D. Redding, H. P. Stahl, R. Webb, O. Alvarez-Salazar, W. L. Arnold, M. Arya, B. Balasubramanian, M. Baysinger, R. Bell, C. Below, J. Benson, L. Blais, J. Booth, R. Bourgeois, C. Bradford, A. Brewer, T. Brooks, E. Cady, M. Caldwell, R. Calvet, S. Carr, D. Chan, V. Cormarkovic, K. Coste, C. Cox, R. Danner, J. Davis, L. Dewell, L. Dorsett, D. Dunn, M. East, M. Effinger, R. Eng, G. Freebury, J. Garcia, J. Gaskin, S. Greene, J. Hennessy, E. Hilgemann, B. Hood, W. Holota, S. Howe, P. Huang, T. Hull, R. Hunt, K. Hurd, S. Johnson, A. Kissil, B. Knight, D. Kolenz, O. Kraus, J. Krist, M. Li, D. Lisman, M. Mandic, J. Mann, L. Marchen, C. Marrese-Reading, J. McCready, J. McGown, J. Missun, A. Miyaguchi, B. Moore, B. Nemati, S. Nikzad, J. Nissen, M. Novicki, T. Perrine, C. Pineda, O. Polanco, D. Putnam, A. Qureshi, M. Richards, A. J. Eldorado Riggs, M. Rodgers, M. Rud, N. Saini, D. Scalisi, D. Scharf, K. Schulz, G. Serabyn, N. Sigrist, G. Sikkia, A. Singleton, S. Shaklan, S. Smith, B. Southerd, M. Stahl, J. Steeves, B. Sturges, C. Sullivan, H. Tang, N. Taras, J. Tesch, M. Therrell, H. Tseng, M. Valente, D. Van Buren, J. Villalvazo, S. Warwick, D. Webb, T. Westerhoff, R. Wofford, G. Wu, J. Woo, M. Wood, J. Ziemer, G. Arney, J. Anderson, J. Maíz-Apellániz, J. Bartlett, R. Belikov, E. Bendek, B. Cenko, E. Douglas, S. Dulz, C. Evans, V. Faramaz, Y. K. Feng, H. Ferguson, K. Follette, S. Ford, M. García, M. Geha, D. Gelino, Y. Götberg, S. Hildebrandt, R. Hu, K. Jahnke, G. Kennedy, L. Kreidberg, A. Isella, E. Lopez, F. Marchis, L. Macri, M. Marley, W. Matzko, J. Mazoyer, S. McCandliss, T. Meshkat, C. Mordasini, P. Morris, E. Nielsen, P. Newman, E. Petigura, M. Postman, A. Reines, A. Roberge, I. Roederer, G. Ruane, E. Schwieterman, D. Sirbu, C. Spalding, H. Teplitz, J. Tumlinson, N. Turner, J. Werk, A. Wofford, M. Wyatt, A. Young, and R. Zellem, "The Habitable Exoplanet Observatory (HabEx) Mission Concept Study Final Report," *arXiv e-prints* , arXiv:2001.06683 (2020).

2 The LUVOIR Team, "The LUVOIR Mission Concept Study Final Report," *arXiv e-prints* , arXiv:1912.06219 (2019).

3 C. C. Stark, R. Belikov, M. R. Bolcar, E. Cady, B. P. Crill, S. Ertel, T. Groff, S. Hildebrandt, J. Krist, P. D. Lisman, J. Mazoyer, B. Mennesson, B. Nemati, L. Pueyo, B. J. Rauscher, A. J. Riggs, G. Ruane, S. B. Shaklan, D. Sirbu, R. Soummer, K. S. Laurent, and N. Zimmerman, "ExoEarth yield landscape for future direct imaging space telescopes," *Journal of Astronomical Telescopes, Instruments, and Systems* **5**, 024009 (2019).

4 R. K. Kopparapu, E. Hébrard, R. Belikov, N. M. Batalha, G. D. Mulders, C. Stark, D. Teal, S. Domagal-Goldman, and A. Mandell, "Exoplanet Classification and Yield Estimates for Direct Imaging Missions," *ApJ* **856**, 122 (2018).

5 S. D. Dulz, P. Plavchan, J. R. Crepp, C. Stark, R. Morgan, S. R. Kane, P. Newman, W. Matzko, and G. D. Mulders, “Joint Radial Velocity and Direct Imaging Planet Yield Calculations. I. Self-consistent Planet Populations,” *ApJ* **893**, 122 (2020).

6 C. C. Stark, A. Roberge, A. Mandell, and T. D. Robinson, “Maximizing the ExoEarth Candidate Yield from a Future Direct Imaging Mission,” *ApJ* **795**, 122 (2014).